Wavelength-Locked 878.6 nm In-Band Pumped Intra-Cavity 2.1 μm Optical Parametric Oscillator *

Shuang Wu(吴爽), Yong-Ji Yu(于永吉)**, Yue Li(李月), Yu-Heng Wang(王宇恒), Jing-Liang Liu(刘景良), Guang-Yong Jin(金光勇)

Jilin Key Laboratory of Solid Laser Technology and Application, College of Science, Changchun University of Science and Technology, Changchun 130022

(Received 23 April 2019)

We report herein a high-power folded intra-cavity 2.1 μm optical parametric oscillator (ICOPO) which is the first example of an ICOPO that utilizes a wavelength-locked 878.6 nm in-band pumped Nd:YVO_4 laser as the pump source. The thermal effect of PPMgLN crystal and the divergence angle of the incident laser are considered comprehensively to determine the 2128 nm degenerate temperature. In the experiment, the functions of different output coupler transmittances and different repetition rates on the parametric laser output power are studied, respectively. The temperature versus parametric laser output power in an in-band pumped non-wavelength-locked 880 nm laser diode (LD) and in a wavelength-locked 878.6 nm LD is compared. A maximum output power of 5.87 W is obtained at the pump power of 56.9 W when the repetition rate is 80 kHz. The corresponding conversion efficiency is 14.55%, with a linewidth of 73.65 nm and pulse width of 3.62 ns. The wavelength-locked 878.6 nm LD in-band pumping technology can stabilize the 2.1 μm laser output power of Nd:YVO_4 crystal effectively in the environment of intense temperature change.

PACS: 42.65.Yj, 42.65.Lm, 42.55.Xi DOI: 10.1088/0256-307X/36/8/084204

Optical parametric oscillators (OPOs) with emission in the eye-safe spectral region around 2 μm play an important role in the fields of atmospheric transmission, remote sensing, laser radar and laser medical treatment as well as in frequency synthesis of mid-IR wavelengths.[1–5] Intra-cavity OPOs (ICOPOs) have exploited the high circulating power by locating the nonlinear medium within the laser resonator, compared to the extra-cavity OPO.[6–10] In recent years, in-band pumping schemes have received increasing attention. Exciting Nd^{3+} ions from the ground state directly to the upper lasing level($^4F_{3/2}$) without the relaxation process of $^4F_{5/2} \rightarrow {}^4F_{3/2}$ can diminish the quantum defect and heat generation effectively. Therefore, better results can be expected if an in-band pumped Nd:YVO_4 laser is used as the pump source of the ICOPO.[11–13]

In this work, we report on a 2.1 μm PPMgLN-ICOPO utilizing an in-band pumped Nd:YVO_4 laser as the pump source. We focus on the influence of the thermal effect of PPMgLN crystal and the divergence angle of the incident laser on the 2128 nm degenerate temperature. We achieve the maximum output power of 5.87 W and the conversion efficiency of 14.55% for Nd:YVO_4 crystal absorption power of 40.33 W at 80 kHz repetition rate with a pulse width of 3.62 ns and a linewidth of 73.65 nm.

A schematic of the experimental setup of the PPMgLN-ICOPO is shown in Fig. 1. In our experiment, the pump source was a 878.6 nm fiber-coupled LD array with a fiber core diameter of 400 μm and an NA of 0.22. The $3\times3\times(5+15)\,mm^3$ a-cut bond composite Nd:YVO_4 crystal consists of two separate sections, i.e. a 15 mm 0.25% Nd^{3+}-doped YVO_4 and a 5 mm undoped cap of YVO_4. Its entrance face was coated for anti-reflection (AR) at 880 nm and high reflection (HR) at 1064 nm. The other face was AR coated at 1064 nm and 880 nm, respectively, to minimize cavity loss and to make the measurement of pump absorption more accurate. The crystal was wrapped with indium foil and mounted in a copper heat sink cooled by an external water-cooler cycle. The multi-lens coupler re-imaged the pump into a Nd:YVO_4 crystal with a ratio of 1:1.5. Pumping the Nd:YVO_4 with a wavelength of 878.6 nm instead of 808 nm helps to reduce the thermal load, hence the maximum pump power allowed was higher. The concave mirror M_3 constitutes the 1064 nm laser oscillating sub-cavity along with the plano mirror M_1. The multiple OPO sub-cavity consists of M_3, a beam splitter (BS) and another concave mirror M_4. The entire double cavity shared a common M_3 mirror and was separated by a BS. A PPMgLN crystal with dimensions of $50\times5\times3\,mm^3$, for which both ends of the faces were AR-coated at 1064 nm and 2.1 μm, was applied as the nonlinear medium. The crystal was mounted into ovens with 0.1℃ accuracy and a temperature range of up to 200℃. The acousto-optic Q-switch was placed between the plano mirrors M_1 and M_2.

According to the calculation of the ABCD matrix, the cavity structure parameters were determined: the 1064 nm laser oscillating sub-cavity length (M_1–M_3)

*Supported by the National Natural Science Foundation of China under Grant No 61505013, the Postdoctoral Science Foundation of China under Grant No 2016M591466, and the Science and Technology Department Project of Jilin Province under Grant Nos 20170204046GX and 20190101004JH.

**Corresponding author. Email: yyjcust@163.com; yuyongji@cust.edu.cn

© 2019 Chinese Physical Society and IOP Publishing Ltd

was set to 375 mm, and the BS was placed 155 mm away from M_2. The multiple OPO sub-cavity length (M_4–M_3) was set to 235 mm, and the BS was 105 mm away from M_3. To maintain the thermal stability of the entire pump and to increase the 1064 nm laser pump intensities in the PPMgLN crystal, a focus lens F was high-transmittance (HT)-coated at 1064 nm with a 150 mm focal length (f = 150 mm), and utilized as an optical ballast to make the 1064 nm laser beam radius insensitive to thermal lens effects and focus the 1064 nm laser waist radius for the purpose of ensuring sufficient pump intensity. It was located close to the Nd:YVO_4 crystal. The specific coating of the cavity mirrors is listed in Table 1.

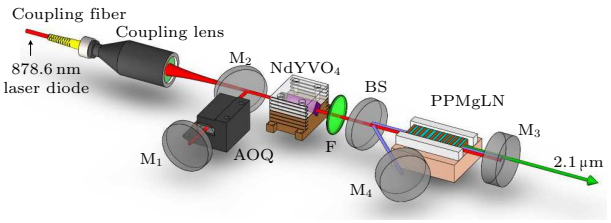

Fig. 1. Experimental setup of the wavelength-locked 878.6 nm in-band pumped 2.1 μm ICOPO.

Table 1. Coating of cavity mirror.

Mirror	Material	Membrane parameter
M_1	K_9	1064 nm@HR
M_2	K_9	880 nm@HT, 1064 nm@HR, 45°angle coating
BS	CaF_2	1064 nm@HT, 2050–2150 nm@HR, 15°angle coating
M_3	CaF_2	1064 nm@HR, 2050–2150 nm@HT (T = 20%, 30%, 50%), Radius of concave (ROC)=−150 mm
M_4	CaF_2	2050–2150 nm@HR ROC=−150 mm

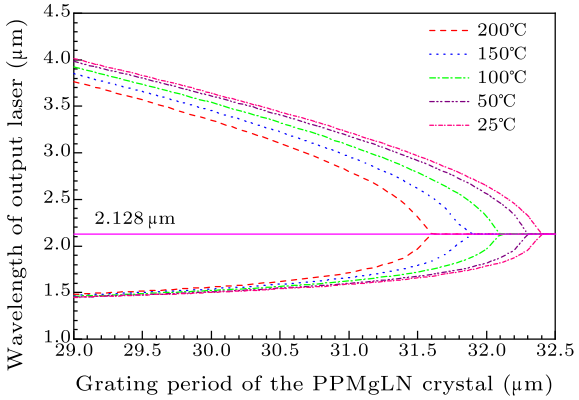

Fig. 2. Grating period and temperature tuning curve of the PPMgLN OPO pumped by a 1064 nm laser.

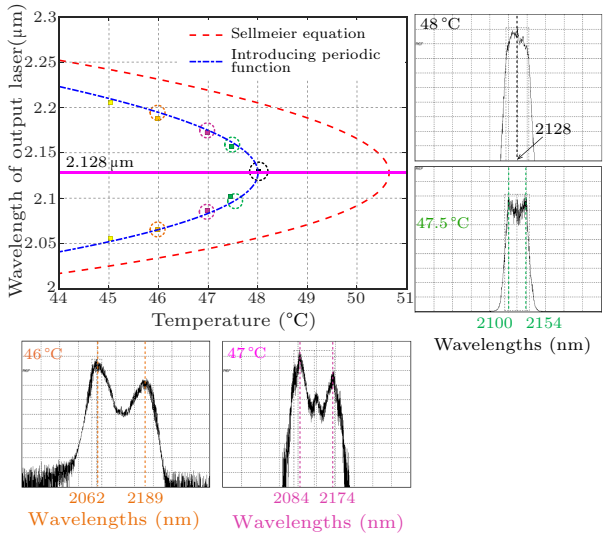

Fig. 3. Experimental wavelengths and the theoretical curve calculated from periodic modulation function.

Since the wavelength of the fundamental beam is determined to be 1064 nm, the degenerate wavelength of the parametric laser is calculated according to the grating period and temperature.[14] Figure 2 shows that the theoretical curve calculated from the Sellmeier equation is simulated by Matlab at different temperatures (25℃, 50℃, 100℃, 150℃, 200℃). The degenerate output of the 2128 nm parametric laser was achieved with a grating period of 31.5–32.5 μm in the temperature range of 25–220℃.

For single-period PPMgLN crystals, the wavelength varies with temperature, and varies most dramatically at the degenerate point. In the experiment, a tunable temperature point is selected to realize the output of 2128 nm degenerate wavelength. The theoretical optimal degenerate temperature should be 50.5℃, much higher than 48℃ in the experiment at 32.25 μm of the grating period. Thus the thermal effect of PPMgLN crystal and the divergence angle of the incident laser must play an important role in this case. We introduce a periodic modulation function[15]

$$\Lambda' = \Lambda + \frac{2\pi}{\sqrt{k_{\rm p}^2 - (k_{\rm p}+k_{\rm s})^2\sin^2\theta - (k_{\rm s}+k_{\rm i})\cos\theta}} \cdot [1+\alpha(T-25)+\beta(T-25)^2],$$

where $k = 2\pi n/\lambda$ represents the wave vector, and θ is the internal divergence angle of the PPMgLN crystal, $\alpha = 1.54\times10^{-5}k^{-1}$ and $\beta = 5.3\times10^{-9}k^{-2}$ are the first- and second-order expansion coefficients along the x-axis, respectively. The expansion coefficients above the third order are very small and negligible. Figure 3 plots the experimental parametric laser wavelengths and the theoretical curve calculated from the periodic modulation function. The optimized wavelength tuning equation agrees well with the measured data.

We first replace M_3 with an output coupler of 48% transmittance at 1064 nm. The 1064 nm fundamental beam output power of 10.39 W was measured when the LD power was 56.9 W with a repetition rate of 80 kHz after the PPMgLN crystal was removed (measured by an F150A-BB-26-PPS power detector produced by

OPHIR Company in Israel), in which the pulse width was 17.4 ns. Then, we discuss the conversion efficiency of the 2.1 μm laser at different transmittance output couplers M_3 and repetition rates. Figure 4 illustrates the 2.1 μm output power as a function of absorbed pump power by Nd:YVO_4 crystal under the three different output couplers (T = 20%, 30%, 50%) at a 80 kHz repetitive rate. The maximum output power was 5.87 W at 2.1 μm when T = 50%. Because of the lower threshold and loss in ICOPO, the parametric laser output power increases with the transmittance under fixed Nd:YVO_4 crystal absorption power.

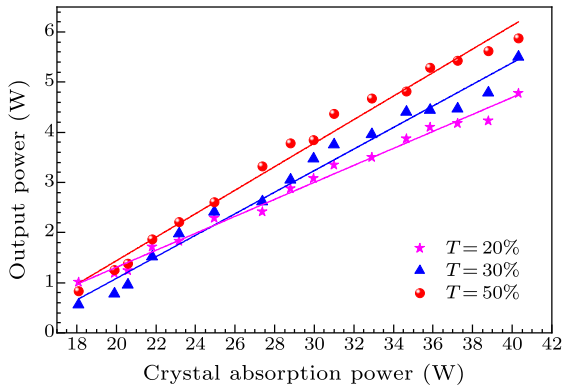

Fig. 4. The 2.1 μm output power versus absorbed pump power by Nd:YVO_4 crystal under different output couplers.

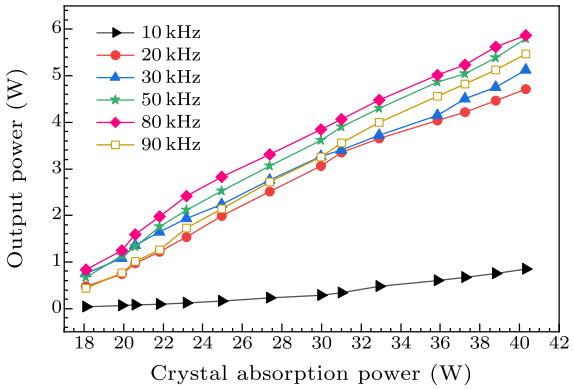

Fig. 5. The T = 50%, 2.1 μm output power versus absorbed pump power by Nd:YVO_4 crystal under different repetition rates.

Using the coupling mirror at the maximum output power mentioned above, the 2.1 μm output power versus absorbed pump power by the Nd:YVO_4 crystal under different repetition rates (10 kHz, 30 kHz, 50 kHz, 60 kHz, 70 kHz, 80 kHz and 90 kHz) can be obtained, as shown in Fig. 5. It is worth pointing out that the output power of 2.1 μm at 10 kHz is much lower than others due to the back-conversion effect caused by the high peak power of the single pulse. When the repetition rate is higher than 80 kHz, the output power of 2.1 μm starts to decrease due to the low peak power of a single pulse and the threshold condition. When the repetition rate is 80 kHz and T = 50%, the maximum output power of 2.1 μm is 5.87 W at the Nd:YVO_4 crystal absorption power of 40.33 W (LD power of 56.9 W), with the conversion efficiency of 14.55% (as shown in Fig. 6).

Shown in Fig. 7 is the 2.1 μm laser output power as a function of the temperature for the 880 nm and wavelength-locked 878.6 nm pumping source. The results show that the wavelength-locked 878.6 nm in-band pumped ICORO in the cases of temperatures 10–40℃ has better power stability than the ICORO traditionally pumped at 880 nm. Since the crystal absorption peak shifts with the temperature change in the wavelength-unlocked case, the conversion efficiency is suppressed and the output power jitters violently.

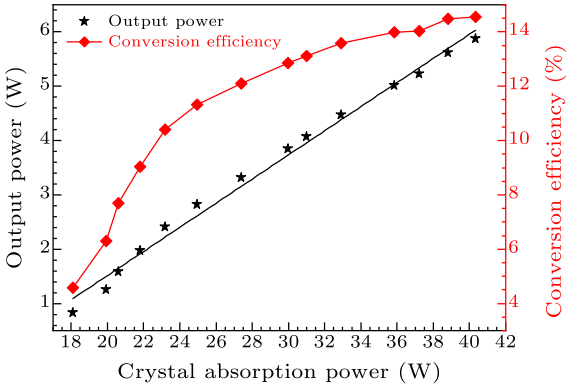

Fig. 6. Repetition rate 80 kHz and T = 50%, 2.1 μm output power and conversion efficiency versus absorbed pump power by Nd:YVO_4 crystal.

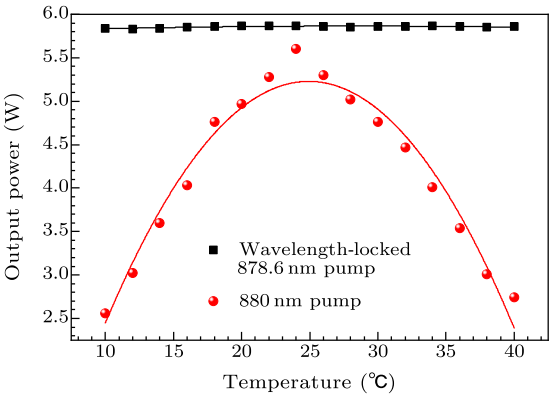

Fig. 7. The 2.1 μm output power as a function of Nd:YVO_4 crystal temperature.

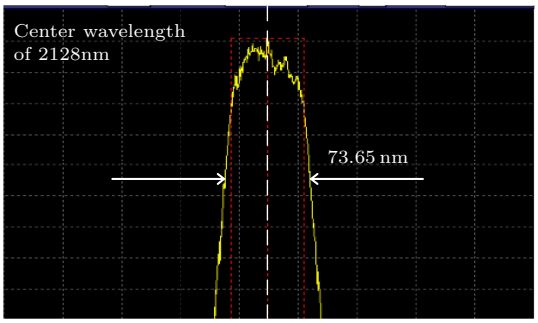

Fig. 8. The spectrum of the 2.1 μm laser at the maximum output power.

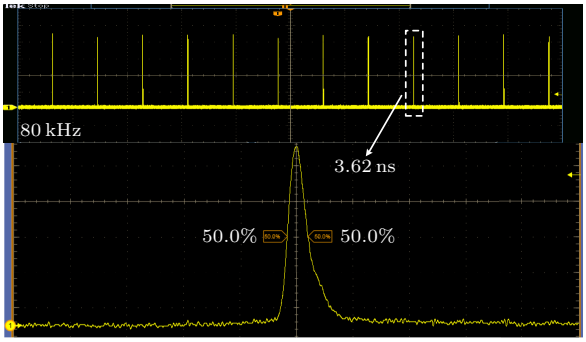

Fig. 9. The pulse sequence and pulse width diagram of the 2128 nm laser.

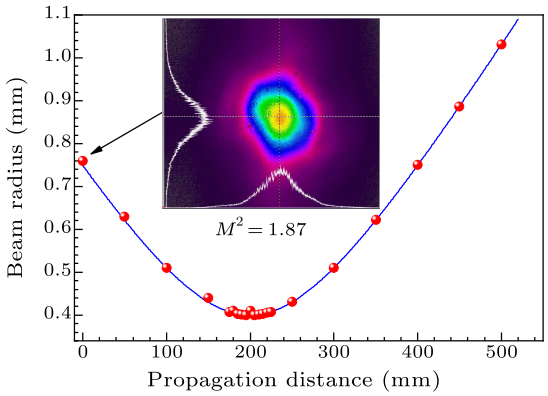

Fig. 10. Measure beam quality factors M^2 of the 2128 nm output laser.

Figure 8 shows the spectrum of the parametric laser at maximum output power with a central wavelength of 2128 nm and a linewidth of 73.65 nm (measured by a YOKOGAWA AQ6375 optical spectrum analyzer with a spectral range of 1.2–2.4 μm). The pulse sequence and pulse width diagram at this time are shown in Fig. 9 (measured by a HgCdTeZn PIC3TE-12 photodetector with a spectral range of 2–10.6 μm). Because of the high gain of the parametric laser and the low photon lifetime of the OPO cavity, the pulse width of 2.1 μm is 3.62 ns, far less than that of 1064 nm.[16] When the Q-switch is turned on, the parametric laser begins to consume the pumped laser energy. Then the pump energy empties rapidly after the peaking power of the parametric laser and reaches parametric laser spontaneous emission below the threshold. It can be seen that accompanied with the increase of the pump consumption induced by higher parametric laser gain, the pulse width narrows faster. Taking the photon loss and round-trip time into the photon lifetime of the OPO cavity, $\tau_{\rm OPO} \approx t_{\rm OPO}/(1-R)$, where R is the reflectivity of output coupling, and $t_{\rm OPO}$ is the round-trip time. The photon lifetime of the 1064 nm laser resonator is $\tau \approx t/(1-\delta)$, where δ is the high-loss factor, and t is the laser resonator round-trip time. Obviously, the photon lifetime of the OPO cavity is much shorter than that of the laser resonator, thus short parametric laser pulses can be obtained. To determine the beam quality factors M^2, using an additional focusing lens ($f = 200$ mm) and a pyroelectric array camera (OPHIR PyrocamⅢ) behind M_3, the radius of 2128 nm laser beams at the maximum output power was measured along the propagation direction after splitting by the 90/10 knife-edge method. Figure 10 shows the evolution of the focused laser beam at different distances from the lens. Derived from Gaussian beam standard propagation expressions, a curve fit to the data yielded $M^2 = 1.87$ for 2128 nm.

In conclusion, we have achieved a high-power PPMgLN-ICOPO based on wavelength-locked 878.6 nm LD in-band pumping, which obtains 2.1 μm parametric laser degenerate output through the grating period and temperature tuning. According to the intra-cavity resonant structure theoretically calculated, the effects of different output coupler transmittances and different repetition rates on the characteristics of the 2.1 μm laser are studied. With a $T = 50\%$ output coupler and 80 kHz repetition rate, the maximum output power is 5.87 W at 2128 nm, corresponding to a conversion efficiency of 14.55%, pulse width of 3.62 ns and linewidth of 73.65 nm. The wavelength-locked 878.6 nm pumped ICOPO achieves 2.1 μm laser output stabilization by diminishing the quantum defect and heat generation effectively at 10–40℃.

References

[1] Wu R F, Phua P B, Lai K S, Lim Y L, Lau E and Chng A 2000 *Opt. Lett.* **25** 1460
[2] Dai S T, Huang J H, Huang H Z, Wu L X, Li J H, Deng J, Ge Y and Lin W X 2017 *Chin. Phys. B* **26** 074211
[3] Cui Q J, Xu Y T, Zong N, Lu Y F, Cheng X K, Peng Q J, Bo Y, Cui D F and Xu Z Y 2009 *Acta Phys. Sin.* **58** 1715 (in Chinese)
[4] Hemming A, Richards J, Davidson A, Carmody N, Bennetts S, Simakov N and Haub J 2013 *Opt. Express* **21** 10062
[5] Wang L, Xing T, Hu S W, Wu X Y, Wu H X, Wang J Y and Jiang H H 2017 *Opt. Express* **25** 3373
[6] Zhu H Y, Zhang G, Lin Y F, Huang C H, Wei Y and Huang L X 2008 *Infrared Laser Eng.* **37** 0054
[7] Peng Y F, Xie G, Wang W M and Wu D Y 2009 *Chin. J. Lasers* **36** 0033
[8] Peng Y F, Xie G, Wang W M and Wu D Y 2009 *Chin. J. Lasers* **36** 2262
[9] Guo J, He G Y, Jiao Z X and Wang B 2015 *Acta Phys. Sin.* **64** 84207 (in Chinese)
[10] Mei J L, Zhong K, Wang M, Liu Y, Xu D, Shi W, Wang Y, Yao J and Liang W 2016 *IEEE Photon. J.* **8** 5502107
[11] Liu Q, Nie M M, Lu F Y and Gong M L 2016 *IEEE Photon. J.* **8** 1502309
[12] Fan H R, Yu Y J, Zu H, Xing S, Wang Y H and Jin G Y 2018 *Infrared Laser Eng.* **47** 606001
[13] Li B, Ding X, Sun B, Sheng Q, Jiang P B, Zhang W, Liu J, Fan C, Zhang H Y and Yao J Q 2014 *Acta Phys. Sin.* **63** 214206 (in Chinese)
[14] Gayer O, Sacks Z, Galun E and Arie A 2008 *Appl. Phys. B* **91** 343
[15] Wang Z J, Yu Y J, Zhai R Z, Chen X Y, Wu C T and Jin G Y 2016 *Laser Phys.* **26** 25401
[16] Falk J, Yarborough J M and Ammann E O 1971 *IEEE J. Quantum Electron.* **7** 359